Fully vectorial highly nonparaxial beam close to the waist

Patrick C. Chaumet

Institut Fresnel (UMR 6133), Université d'Aix-Marseille III, Avenue Escadrille Normandie-Niemen, F-13397 Marseille Cedex 20, France

Received May 5, 2006; accepted June 1, 2006; posted July 6, 2006 (Doc. ID 70545)

I use the angular spectrum representation to compute exactly the Gaussian beam close to the waist (w_0) in the case of a highly nonparaxial field ($w_0 < \lambda$). The computation is done in the vectorial case for a polarized Gaussian beam. In the area of the waist, the contribution of the propagating and evanescent waves is discussed. Moreover, the Gaussian wave is developed in terms of a series, which permits one to get analytical expressions for both propagating and evanescent waves when the observation is close to the waist. © 2006 Optical Society of America

OCIS codes: 350.5500, 260.1960, 260.2110.

1. INTRODUCTION

The beam propagation beyond the paraxial region has been extensively studied.[1–4] In the past decade, the vectorial Gaussian beam has been studied in the regime of a waist width (w_0) smaller than the wavelength.[5–9] Highly nonparaxial beams can be very useful in many areas in physics, for example, in performing optical trapping and optical manipulation,[10,11] or in optical diffraction tomography where a highly focused beam permits one to reduce the investigation domain.[12]

In the case of a highly focused beam with a waist width smaller than the wavelength, the study is always done far from the waist with, for example a power-series expansion for the transverse field[6] or longitudinal field,[5] hence the evanescent waves are not taken into account. In this paper I focus on the waist area, which implies that the evanescent waves are not negligible and should be computed correctly. Hence I use an angular spectrum representation,[13] which permits one to separate the contribution of the evanescent and propagating waves without approximation. Then, by using a Taylor series, I express the electric field in an analytic form when the observation point is close to the waist. The advantages of this analytic formulation, not previously derived to my knowledge, are its speed, and the ease with which one can compare the weight of the evanescent and propagating waves.

The paper is organized as follows. In Subsection 2.A the definition and notation used in the problem are given. Subsection 2.B develops the theory to compute separately the evanescent and propagating waves without approximation as well as an analytical form when the observation is close to the waist. Section 3 is devoted to the results, and Section 4 presents the conclusions.

2. THEORY

A. Position of the Problem

To describe a polarized Gaussian beam, I use the well-known angular spectrum representation in the Cartesian coordinate system.[13] Omitting the dependence in $i\omega t$, the electric field can be expressed as

$$E_x(\mathbf{r}) = \int_{-\infty}^{+\infty}\int_{-\infty}^{+\infty} A_x(k_x,k_y)\exp[\mathrm{i}(k_x x + k_y y + k_z z)]\mathrm{d}k_x\mathrm{d}k_y, \tag{1}$$

$$E_y(\mathbf{r}) = \int_{-\infty}^{+\infty}\int_{-\infty}^{+\infty} A_y(k_x,k_y)\exp[\mathrm{i}(k_x x + k_y y + k_z z)]\mathrm{d}k_x\mathrm{d}k_y, \tag{2}$$

$$E_z(\mathbf{r}) = -\int_{-\infty}^{+\infty}\int_{-\infty}^{+\infty}\left[\frac{k_x}{k_z}A_x(k_x,k_y) + \frac{k_y}{k_z}A_y(k_x,k_y)\right] \times\exp[\mathrm{i}(k_x x + k_y y + k_z z)]\mathrm{d}k_x\mathrm{d}k_y, \tag{3}$$

in the $z>0$ half-space, where the z axis is taken to be the direction of propagation. The wave vector has a magnitude $k_0^2=(\omega/c)^2=k_x^2+k_y^2+k_z^2$ with

$$k_z = \sqrt{(k_0^2 - k_x^2 - k_y^2)} \quad \text{for propagating waves}, \tag{4}$$

$$k_z = i\sqrt{(k_x^2 + k_y^2 - k_0^2)} \quad \text{for evanescent waves}. \tag{5}$$

To find the coefficients A_x and A_y, the initial guess taken for the field at $z=0$ evolves from that of Agrawal and Pattanayak[6]

$$E_x(x,y,0) = E_{0x}\exp\left(-\frac{\rho^2}{2w_0^2}\right), \tag{6}$$

$$E_y(x,y,0) = E_{0y}\exp\left(-\frac{\rho^2}{2w_0^2}\right), \tag{7}$$

with $\rho^2=x^2+y^2$, w_0 is the waist of the Gaussian beam, and E_{0x} and E_{0y} are the magnitudes of the Gaussian beam at the origin for the x and y components, respectively. Using the inverse Fourier transform, it is easy to find

$$A_l(k_x,k_y) = E_{0l}\frac{w_0^2}{2\pi}\exp\left(-\frac{k^2w_0^2}{2}\right), \tag{8}$$

where l stands for either x or y, and $k^2=k_x^2+k_y^2$. Since the Gaussian beam is invariant under rotation about the z axis, we will work with polar coordinates rather than Cartesian coordinates. Replacing $\mathrm{d}k_x\mathrm{d}k_y$ with $k\mathrm{d}k\mathrm{d}\theta$ and performing the angular integration introduces the zeroth and first-order Bessel function of the first kind, so as to yield

$$E_l(\mathbf{r}) = E_{0l}I_x(\mathbf{r}), \tag{9}$$

$$I_x(\mathbf{r}) = \int_0^{+\infty} w_0^2 f(k)\exp(\mathrm{i}k_z z)J_0(k\rho)k\mathrm{d}k, \tag{10}$$

$$E_z(\mathbf{r}) = -i(\sin\theta E_{0x} + \cos\theta E_{0y})I_z(\mathbf{r}), \tag{11}$$

$$I_z(\mathbf{r}) = \int_0^{+\infty} \frac{k^2w_0^2}{k_z} f(k)\exp(\mathrm{i}k_z z)J_1(k\rho)\mathrm{d}k, \tag{12}$$

with $f(k)=\exp[-(k^2w_0^2/2)]$, $\sin\theta=x/\rho$, and $\cos\theta=y/\rho$. At this step, generally, one studies the behavior of the propagating waves by performing power-series expansion for the transverse field[6] or longitudinal field[5] when z is large compared to the wavelength. Afterwards one usually[5,6] compares the different terms of the series to the usual paraxial or spherical approximation. In our case, we are interested in studying the field close to the waist and in comparing, in this area, the contribution of the propagating and evanescent waves.

B. Contribution of Evanescent and Propagating Waves: Study Close to the Waist

We want to know the contribution of evanescent and propagating waves, hence we should separate the integration performed over k as $\int_0^{+\infty}=\int_0^{k_0}+\int_{k_0}^{+\infty}$, where the first and second integrations correspond, respectively, to the propagating and evanescent waves. To avoid the problem that occurs at $k=k_0$ (which implies $k_z=0$) for I_z, I perform the integration over the normal component of the wave vector. Hence, one can write

$$I_x(\mathbf{r}) = \left(\int_0^{k_0} - \int_0^{+i\infty}\right) w_0^2 f(k)\exp(\mathrm{i}k_z z)J_0(k\rho)k_z\mathrm{d}k_z, \tag{13}$$

$$I_z(\mathbf{r}) = \left(\int_0^{k_0} - \int_0^{+i\infty}\right) w_0^2 f(k)\exp(\mathrm{i}k_z z)J_1(k\rho)k\mathrm{d}k_z. \tag{14}$$

In a more detailed form Eqs. (13) and (14) become

$$I_{x,\mathrm{pro}}(\mathbf{r}) = \int_0^{k_0} w_0^2\exp\left(-\frac{w_0^2(k_0^2-k_z^2)}{2}\right) \times\exp(\mathrm{i}k_z z)J_0\left(\rho\sqrt{k_0^2-k_z^2}\right)k_z\mathrm{d}k_z, \tag{15}$$

$$I_{x,\mathrm{eva}}(\mathbf{r}) = \int_0^{\infty} w_0^2\exp\left(-\frac{w_0^2(k_0^2+\alpha^2)}{2}\right) \times\exp(-\alpha z)J_0\left(\rho\sqrt{k_0^2+\alpha^2}\right)\alpha\mathrm{d}\alpha, \tag{16}$$

$$I_{z,\mathrm{pro}}(\mathbf{r}) = \int_0^{k_0} w_0^2\exp\left(-\frac{w_0^2(k_0^2-k_z^2)}{2}\right) \times\exp(\mathrm{i}k_z z)J_1\left(\rho\sqrt{k_0^2-k_z^2}\right)\sqrt{k_0^2-k_z^2}\mathrm{d}k_z, \tag{17}$$

$$I_{z,\mathrm{eva}}(\mathbf{r}) = -i\int_0^{\infty} w_0^2\exp\left(-\frac{w_0^2(k_0^2+\alpha^2)}{2}\right) \times\exp(-\alpha z)J_1\left(\rho\sqrt{k_0^2+\alpha^2}\right)\sqrt{k_0^2+\alpha^2}\mathrm{d}\alpha, \tag{18}$$

where the indices "eva" and "pro" mean that the integration corresponds to the evanescent and propagating waves, respectively. One can note from Eqs. (16) and (18) that the integration that represents the evanescent waves is real for the x component and imaginary for the z component. Equations (15)–(18) can be evaluated numerically and hence we can obtain the field without any approximation at any position $\mathbf{r}$. To my knowledge, this is the first time that the evanescent part of a Gaussian beam is presented. To the best of my knowledge, one can note only one recent work that separates the evanescent and propagating parts in expanding the electric field to the modal function, but in the scalar case.[14]

The integrations represented by Eqs. (15)–(18) can be inconvenient to perform, and in the case where the observation point is close to the z axis, we can use a more efficient approach. We are interested in the electric field in the waist area with a waist width smaller than the wavelength. Hence when ρ increases, the electric field vanishes very quickly. Then the Bessel functions, $J_0(k\rho)$ and $J_1(k\rho)$, can be written in terms of series with the argument $k\rho$.[15] Moreover using the binomial theorem, Eqs. (13) and (14) are rewritten as

$$I_x(\mathbf{r}) = w_0^2 f(k_0)\sum_{l=0}^{\infty} C_l \sum_{m=0}^{l} \frac{(-1)^m}{k_0^{2m} m!\,(l-m)!}\left(\int_0^{k_0} - \int_0^{+i\infty}\right) \times\exp\left(k_z^2\frac{w_0^2}{2}\right)\exp(\mathrm{i}k_z z)k_z^{2m+1}\mathrm{d}k_z, \tag{19}$$

$$I_z(\mathbf{r}) = w_0^2 f(k_0)\frac{\rho k_0^2}{2}\sum_{l=0}^{\infty} C_l \sum_{m=0}^{l+1} \frac{(-1)^m}{k_0^{2m} m!\,(l+l-m)!} \times\left(\int_0^{k_0} - \int_0^{+i\infty}\right)\exp\left(k_z^2\frac{w_0^2}{2}\right) \times\exp(\mathrm{i}k_z z)k_z^{2m}\mathrm{d}k_z, \tag{20}$$

with $C_l=[(-1)^l(k_0\rho)^{2l}]/4^l l!$. Now each integration can be easily evaluated as Eqs. (19) and (20) can be computed using the following relations[16]

$$I_{m,\mathrm{eva}} = \int_0^{+i\infty} \exp\left(\frac{k_z^2 w_0^2}{2}\right)\exp(\mathrm{i}k_z z)k_z^m \mathrm{d}k_z = \frac{i^{m+1}m!}{w_0^{m+1}} D_{m+1}\left(\frac{z}{w_0}\right), \quad (21)$$

for the evanescent part with

$$D_1\left(\frac{z}{w_0}\right) = \sqrt{\frac{\pi}{2}} w\left(\frac{iz}{\sqrt{2}w_0}\right), \quad (22)$$

$$D_2\left(\frac{z}{w_0}\right) = 1 - \frac{z}{w_0} D_1\left(\frac{z}{w_0}\right), \quad (23)$$

$$D_{m+1}\left(\frac{z}{w_0}\right) = \frac{1}{m}\left[D_{m-1}\left(\frac{z}{w_0}\right) - \frac{z}{w_0} D_m\left(\frac{z}{w_0}\right)\right], \quad (24)$$

where D is related to the parabolic cylinder function. For the integration representing the propagating part, we get

$$I_{m,\mathrm{pro}} = \int_0^{k_0} \exp\left(\frac{k_z^2 w_0^2}{2}\right)\exp(\mathrm{i}k_z z)k_z^m \mathrm{d}k_z = \exp\left(\frac{w_0^2 k_0^2}{2}\right)\exp(\mathrm{i}k_0 z)\frac{k_0^{m-1}}{w_0^2} - \frac{iz}{w_0^2} I_{m-1,\mathrm{pro}} - \frac{m-1}{w_0^2} I_{m-2,\mathrm{pro}}, \quad (25)$$

with

$$I_{1,\mathrm{pro}} = \frac{1}{w_0^2}\left[\exp\left(\frac{w_0^2 k_0^2}{2}\right)\exp(\mathrm{i}k_0 z) - 1 - iz I_{0,\mathrm{pro}}\right], \quad (26)$$

$$I_{0,\mathrm{pro}} = \frac{i}{w_0}\sqrt{\frac{\pi}{2}}\left[w\left(\frac{iz}{\sqrt{2}w_0}\right) - \exp\left(\frac{w_0^2 k_0^2}{2}\right) \times \exp(\mathrm{i}k_0 z) w\left(\frac{iz}{w_0\sqrt{2}} + \frac{w_0 k_0}{\sqrt{2}}\right)\right]. \quad (27)$$

$w(\cdot)$ is the Faddeev function and can be computed in a very efficient way.[17] In conclusion, computing Eqs. (19) and (20) does not require a numerical effort as one needs only to compute the Faddeev function with two different arguments and use relations of recurrence. As an example we give below the first term of the series, i.e., $l=0$

$$I_{x,\mathrm{eva}}(\mathbf{r}) = f(k_0)\left[1 - \frac{z}{w_0}\sqrt{\frac{\pi}{2}} w\left(\frac{iz}{\sqrt{2}w_0}\right)\right], \quad (28)$$

$$I_{x,\mathrm{pro}}(\mathbf{r}) = \exp(\mathrm{i}zk_0)\left[1 - \frac{z}{w_0}\sqrt{\frac{\pi}{2}} w\left(\frac{iz}{w_0\sqrt{2}} + \frac{w_0 k_0}{\sqrt{2}}\right)\right] - I_{x,\mathrm{eva}}(\mathbf{r}), \quad (29)$$

$$I_{z,\mathrm{eva}}(\mathbf{r}) = \frac{i\rho}{2w_0^2} f(k_0)\left[z - \sqrt{\frac{\pi}{2}}\left(\frac{w_0^4 k_0^2 + z^2 + w_0^2}{w_0}\right) w\left(\frac{iz}{\sqrt{2}w_0}\right)\right], \quad (30)$$

$$I_{z,\mathrm{pro}}(\mathbf{r}) = \frac{\rho}{2}\exp(\mathrm{i}zk_0)\left[-k_0 + \frac{iz}{w_0^2} - i\sqrt{\frac{\pi}{2}}\left(\frac{w_0^4 k_0^2 + z^2 + w_0^2}{w_0^3}\right) w\left(\frac{iz}{w_0\sqrt{2}} + \frac{w_0 k_0}{\sqrt{2}}\right)\right] - I_{z,\mathrm{eva}}(\mathbf{r}). \quad (31)$$

Notice that when z becomes large compared to the wavelength Eqs. (28)–(31) can be written in terms of a power-series expansion in $1/z$:

$$I_{x,\mathrm{eva}}(\mathbf{r}) = \frac{w_0^2}{z^2} f(k_0) + O\left(\frac{1}{z^4}\right), \quad (32)$$

$$I_{x,\mathrm{pro}}(\mathbf{r}) = -i\frac{w_0^2 k_0}{z}\exp(\mathrm{i}zk_0) + O\left(\frac{1}{z^2}\right), \quad (33)$$

$$I_{z,\mathrm{eva}}(\mathbf{r}) = -\rho\frac{ik_0^2 w_0^2}{2z} f(k_0) + O\left(\frac{1}{z^3}\right), \quad (34)$$

$$I_{z,\mathrm{pro}}(\mathbf{r}) = \rho\frac{ik_0^2 w_0^2}{2z} f(k_0) - \rho\frac{w_0^2 k_0}{z^2}\exp(\mathrm{i}zk_0) + O\left(\frac{1}{z^3}\right). \quad (35)$$

Hence, one can note that for the z component, the first non-null term is the $1/z$ term for both evanescent and propagating waves. Therefore, it seems that the evanescent waves contribute to the far field as the propagating term. Incidentally, a few years ago, there were some claims as to the contribution of evanescent waves to the power radiated to the far field by a dipolar source.[18] The $1/z$ term is a mathematical artifact associated with the choice of a particular plane with respect to which the angular spectrum representation is derived. From a physical point of view, no energy is carried to the far field by the evanescent modes of the field and the only physically sound quantity in the far field is the total field which is, for all practical purposes, propagating.[19–21] Then, one can see that the total field, i.e., $I_{x,\mathrm{eva}}+I_{x,\mathrm{pro}}$ and $I_{z,\mathrm{eva}}+I_{z,\mathrm{pro}}$, matches perfectly the first term of the power-series expansion of the transverse and longitudinal field presented in Ref. 5 with the approximation that z is large compared to the wavelength and ρ is close to zero.

3. NUMERICAL RESULTS

In this section, I present some results computed in the waist area for a waist smaller than the wavelength. Figure 1 presents the propagating and evanescent parts for the x and z components of the electric field for a Gaussian beam with a waist of $w_0=\lambda/2$. The polarization

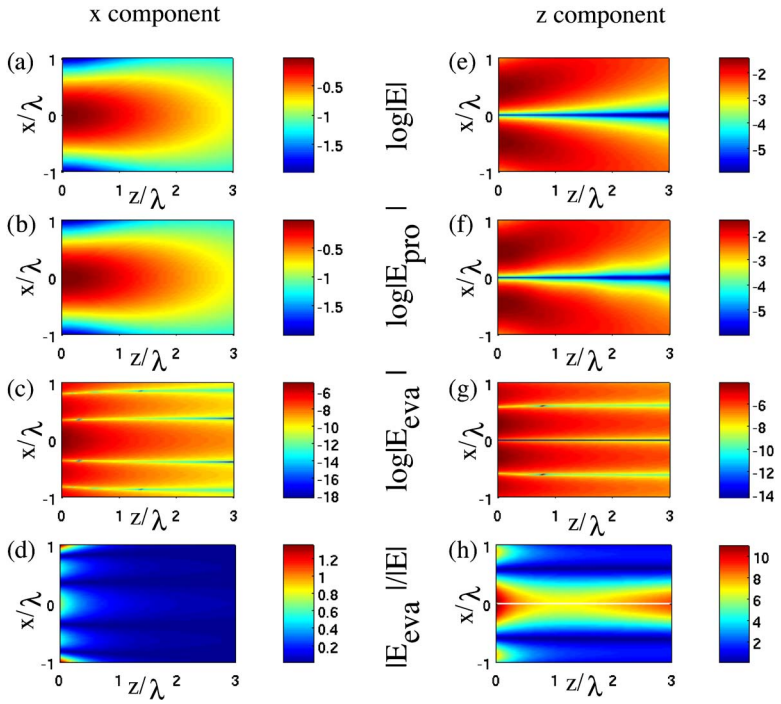

Fig. 1. (Color online) Gaussian beam with $w_0=\lambda/2$ in the (x,z) plane at $y=0$. The left- and right-side are on the x and z components, respectively. (a) and (e) are the logarithm of the modulus of the component of the electric field. (b) and (f) are the logarithms of the modulus of the propagating part, (c) and (g) are the logarithms of the modulus of the evanescent part, (d) and (h) are the ratios in percent between the modulus of the evanescent part and the modulus of the total electric field.

of the Gaussian beam is such as $E_{0y}=0$, $E_{0x}=1$, and the field is presented in the plane (x,z) at $y=0$. Note that in Figs. 1(a)–1(c) and 1(e)–1(g), we present the logarithm of the components (detailed in the legend of the figure) in order to appreciate more easily their variations.

No qualitative difference emerges from Figs. 1(a) and 1(b), and Figs. 1(e) and 1(f) between the modulus of the electric field E_x and E_z and the modulus of the propagating part i.e., $E_{x,\mathrm{pro}}$ and $E_{z,\mathrm{pro}}$, respectively. One can notice that the z component of the electric field vanishes on the z axis. Figures 1(c) and 1(g) present the evanescent part for the x component and z component, respectively, and when $z>\lambda$ they exhibit a dark horizontal line that denotes a strong decrease of both components. To my knowledge, this effect has not previously been commented upon. When we look carefully at the expressions of the evanescent part, Eqs. (16) and (18), they contain the terms $\exp(-\alpha z)J_0(\rho\sqrt{k_0^2+\alpha^2})$ and $\exp(-\alpha z)J_1(\rho\sqrt{k_0^2+\alpha^2})$ for the x and z components, respectively. When z increases, $\exp(-\alpha z)$ decays very quickly and only α close to zero gives a significant contribution to the integral. Hence, when ρ is such as $J_0(\rho k_0)=0$ the x component vanishes, and when ρ is such as $J_1(\rho k_0)=0$ the z component vanishes: this explains the dark line in Figs. 1(c) and 1(g). Figures 1(d) and 1(h) represent the ratio, in percentage, between the modulus of the evanescent part of the electric field and the modulus of the electric field, i.e., $100|E_{x,\mathrm{eva}}|/|E_x|$ for Fig. 1(d) and $100|E_{z,\mathrm{eva}}|/|E_z|$ for Fig. 1(h). As expected, Fig. 1(d) shows that for the transverse component the contribution of the evanescent waves for $z>\lambda$ is less than 0.5%, thus it is perfectly negligible compared to the propagating waves. In the case of the longitudinal component, Fig. 1(h), the relative difference is strong for a small value of z when the electric field is computed close to the waist, and large for a value of z due to a mathematical artifact as explained previously in Subsection 2.B.

We study the same Gaussian beam as in Fig. 1 but in the plane (x,y) close to the waist. i.e., at $z=\lambda/4$. As previously observed, at first view there is little difference between the modulus of the electric field with its propagating components [Figs. 2(a) and 2(b)]. In Figs. 2(c) and 2(g) the evanescent component shows circles due to, as previously stated, the Bessel function. For the z component note that it vanishes for $y=0$. Figures 2(d) and 2(h) show that the error made if the evanescent waves are not taken into account increases drastically for both components when the observation becomes far from the z axis, i.e., $\rho>\lambda=2w_0$.

Figure 3 compares the exact solution obtained from Eqs. (15)–(18) (crosses) and the series described by Eqs. (19) and (20) versus x. The cutoff for the series is done at $l=10$ (solid curve) and $l=30$ (dashed curve). One can note that when x increases, it is necessary to compute the series for higher values of l, but for a small value of x, the series is a rapid way to obtain the components of the electric field.

Figure 4 studies the effect of the distance z, and of the waist on both components. As expected, when the distance z increases, the evanescent waves decrease for both waists. Note that the oscillations of the evanescent component are due to the Bessel function as explained previously, which means they do not depend on the waist width. The only effect of the waist on the evanescent waves is to lower their magnitude, but the shape stays the same. For the propagating waves, the effect of the

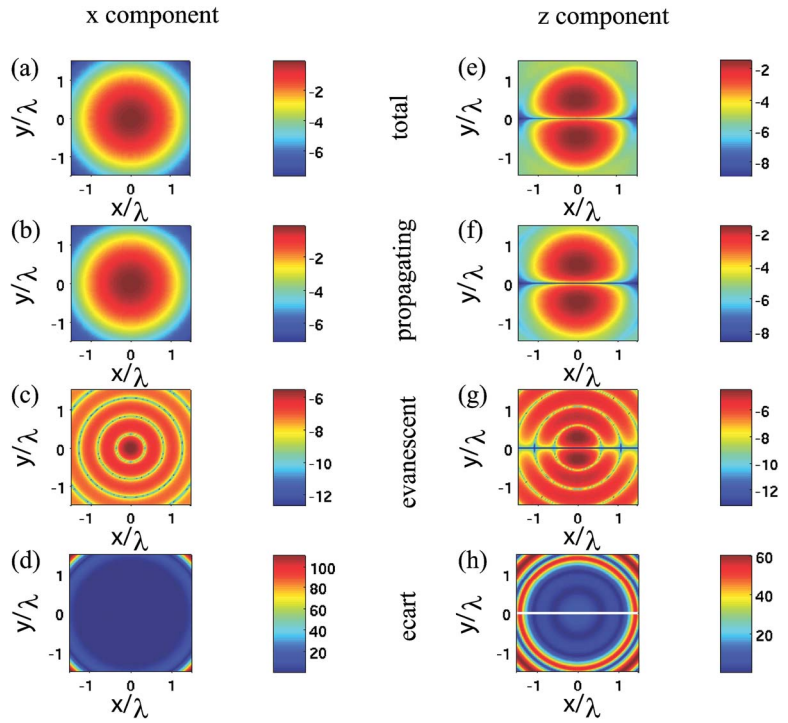

Fig. 2. (Color online) Gaussian beam with $w_0=\lambda/2$ in the (x,y) plane at $z=\lambda/4$. Same legend as in Fig. 1.

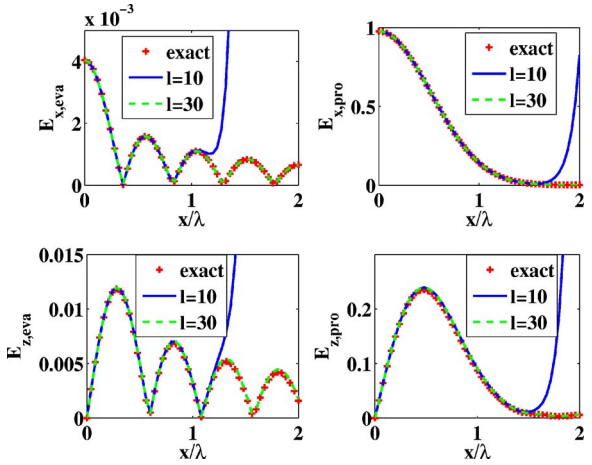

Fig. 3. (Color online) Gaussian beam with $w_0=\lambda/2$ versus x/λ at $z=\lambda/4$. With crosses the exact solution using Eqs. (15)–(18). Solid curve and dashed curve with the series development with $l=10$ and $l=30$, respectively. (a) x component for the evanescent wave. (b) x component for the propagating wave. (c) z component for the evanescent wave. (d) z component for the propagating wave.

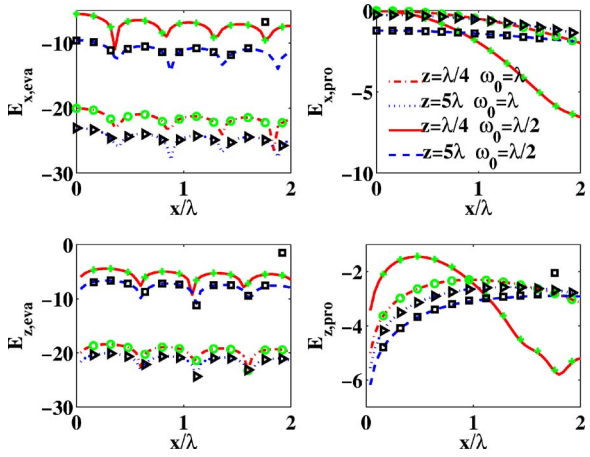

Fig. 4. (Color online) Gaussian beam with $w_0=\lambda/2$ versus x/λ at $z=\lambda/4$ in the solid curve and $z=5\lambda$ in the dashed curve and with $w_0=\lambda$ at $z=\lambda/4$ in the dot-dashed curve and $z=5\lambda$ in the dotted curve. Note that the symbols are the results of the series development with $l=30$. (a) x is the component for the evanescent wave. (b) x is the component for the propagating wave. (c) z is the component for the evanescent wave. (d) z component for the propagating wave.

waist is obvious and well known. Notice that the series associated with the propagating waves converge more quickly than those associated with the evanescent waves.

Table 1 presents some results on the convergence of the series expansion of Eqs. (19) and (20) versus w_0, ρ, and z. It shows that when the waist increases, the convergence is easier. When ρ increases, the convergence is more difficult. This is because the Bessel function is developed in a Taylor series in a power of ρ. Regarding z, a larger value will give a quicker convergence when we are close to the waist, but this is no longer the case for high values of $z(z>100\lambda)$, because in that case it does not make any

Table 1. Value of l Needed to Compute I_x and I_z[a]

	$\rho=\lambda/4$		$\rho=\lambda/2$		$\rho=\lambda$	
	$z=\lambda/4$	$z=\lambda$	$z=\lambda/4$	$z=\lambda$	$z=\lambda/4$	$z=\lambda$
$w_0=\lambda/4$	3 (2)	3 (2)	7 (4)	5 (4)	21 (8)	11 (8)
$w_0=\lambda/2$	3 (2)	3 (2)	5 (3)	5 (3)	10 (7)	9 (7)
$w_0=\lambda$	3 (2)	3 (2)	5 (2)	5 (2)	9 (3)	9 (3)

[a]Value of l needed in Eqs. (19) and (20) to compute I_x and I_z (propagating and evanescent waves) with a precision smaller than 1% compared to the exact solution computed through Eqs. (15)–(18). Between brackets, the value of l is needed only for the propagating waves to reach the precision wished.

sense to take our formulation, and a series expansion in $1/z$ (Refs. 5 and 6) would be preferable.

4. CONCLUSION

In this paper, I compute the longitudinal and transverse components for a fully vectorial, highly nonparaxial beam without approximation. I separate the contribution from the evanescent and propagating waves and study the importance of the evanescent waves close to the waist. I note some oscillations of the evanescent waves versus ρ that are independent of the waist and the distance z (for $z > \lambda$) and give analytical expressions of the evanescent and propagating waves when the point of observation is close to the waist.

ACKNOWLEDGMENTS

The author thanks Adel Rahmani for useful correspondence concerning the angular spectrum representation, and S. Vajk for a careful reading of the manuscript.

The author may be contacted by e-mail at patrick.chaumet@fresnel.fr.

REFERENCES

1. M. Lax, W. H. Louisell, and W. B. McKnight, "From Maxwell to paraxial wave optics," Phys. Rev. A **11**, 1365–1370 (1975).
2. L. W. Davis, "Theory of electromagnetic beams," Phys. Rev. A **19**, 1177–1179 (1979).
3. G. P. Agrawal and M. Lax, "Free-space wave propagation beyond the paraxial approximation," Phys. Rev. A **27**, 1693–1695 (1983).
4. C. J. R. Sheppard and S. Saghafi, "Electromagnetic Gaussian beams beyond the paraxial approximation," J. Opt. Soc. Am. A **16**, 1381–1386 (1999).
5. C. G. Chen, P. T. Konkola, J. Ferrera, R. K. Heilmann, and M. L. Schattenburg, "Analyses of vector Gaussian beam propagation and the validity of paraxial and spherical approximation," J. Opt. Soc. Am. A **19**, 404–412 (2002).
6. G. P. Agrawal and D. N. Pattanayak, "Gaussian beam propagation beyond the paraxial approximations," J. Opt. Soc. Am. **69**, 575–578 (1979).
7. G. Zhou, X. Chu, and L. Zhao, "Propagation characteristics of TM Gaussian beam," Opt. Laser Technol. **37**, 470–474 (2005).
8. A. Ciattoni, B. Crosignani, and P. Di Porto, "Vectorial analytical description of propagation of a highly nonparaxial beam," Opt. Commun. **202**, 17–20 (2002).
9. K. Duan and B. Lü, "Polarization properties of vectorial nonparaxial Gaussian beams in the far field," Opt. Lett. **30**, 309–310 (2005).
10. A. Ashkin, "Trapping of atoms by resonance radiation pressure," Phys. Rev. Lett. **40**, 729–732 (1978).
11. A. Ashkin, "Optical trapping and manipulation of neutral particles using lasers," Proc. Natl. Acad. Sci. U.S.A. **94**, 4853–4860 (1997).
12. K. Belkebir, P. C Chaumet, and A. Sentenac, "Influence of multiple scattering on three-dimensional imaging with optical diffraction tomography," J. Opt. Soc. Am. A **23**, 586–595 (2006).
13. L. Mandel and E. Wolf, *Optical Coherence and Quantum Optics* (Cambridge U. Press, 1995), p. 109.
14. N. I. Petrov, "Evanescent and propagating fields of a strongly focused beam," J. Opt. Soc. Am. A **20**, 2385–2389 (2003).
15. I. S. Gradshteyn and I. M. Ryzhik, *Table of Integrals, Series and Products, Corrected and Enlarged Edition* (Academic, 1980), p. 951.
16. I. S. Gradshteyn and I. M. Ryzhik, *Table of Integrals, Series and Products, Corrected and Enlarged Edition* (Academic, 1980), pp. 1064–1067.
17. G. P. M. Poppe and C. M. J. Wijers, "More efficient computation of the complex error function," ACM Trans. Math. Softw. **16**, 38–46 (1990).
18. M. Xiao. "Evanescent waves do contribute to the far field," J. Mod. Opt. **46**, 729–733 (1999).
19. E. Wolf and J. Foley, "Do evanescent waves contribute to the far field?" Opt. Lett. **23**, 16–18 (1998).
20. A. Rahmani and G. W. Bryant, "Contribution of evanescent waves to the far field: the atomic point of view," Opt. Lett. **25**, 433–435 (2000).
21. T. Setälä, M. Kaivola, and A. Friberg, "Evanescent and propagating electromagnetic fields in scattering from point-dipole structures: reply to comment," J. Opt. Soc. Am. A **19**, 1449–1451 (2002).